Silicon pore optics for high-energy optical systems

Girou, D.A.

3

PLASMA ETCHING FOR THE COMPATIBILITY OF THIN FILM METALLIC COATINGS AND DIRECT BONDING OF SILICON PORE OPTICS

Silicon pore optics are a new type of high-performance X-ray optics designed to enable future space-borne X-ray observatories such as ESA's Athena. These optics will make it possible to build telescopes with effective areas of the order of a few square meters and angular resolutions better than 5 seconds of arc. During manufacturing of the optics, thin film metallic coatings are sputtered onto mirror plates to help achieve this large effective area. Then these plates are stacked on top of each other using direct silicon bonding to achieve the shape of an approximate Wolter type-I telescope design. It is therefore necessary to verify the compatibility of the coating and bonding processes. We observe the unintentional removal of coatings on silicon pore optics plates after their wet chemical activation, a step required to make direct bonding possible. In this chapter we investigate plasma etching prior to thin film deposition as a solution to this problem. First we ensure that plasma etching does not impact the low surface roughness required to achieve high imaging performance. Then we demonstrate that plasma etching before thin film deposition prevents unintentional removal of the metallic coatings during the activation step, making coating deposition compatible with direct bonding of silicon pore optics plates.

Parts of this chapter have been published in the Journal of Applied Physics **128**, 095302 (2020) [1].

3.1 Introduction

As the development of SPO progresses, it is necessary to validate the direct bonding process with the metallic coating deposition process needed for the observatory to achieve a large effective area [2]. The coating deposition process consists in sputtering thin films of metals onto the non-ribbed side of an SPO plate while a patterned photoresist layer prevents the coating from depositing onto the bonding surfaces. The photoresist is then lifted off chemically and the bonding surfaces are cleaned using an RCA recipe [3] (SC-1 cleaning only). Previous studies observed unintentional removal of metallic thin films on SPO after the wet chemical cleaning step required for the direct bonding and indicated that molecular contamination originating from the ambient as well as from fabrication processes such as photoresist remnants might be the cause [4]. Surface treatment is therefore considered to provide clean surfaces prior to thin film deposition and reduce coating surface defects. An inverse sputter etcher (ISE) unit has been implemented in the DC magnetron sputtering machine dedicated for the SPO production [5]. After photoresist deposition this ISE allows for plasma cleaning of the substrate surfaces in situ, before thin film deposition. This way, vacuum is maintained between the plasma etching and coating processes, preventing the substrates to be exposed to the atmosphere. The etching process is performed by bombarding the SPO plate surface with a mixture of argon and oxygen ions. Possible organic contamination and photoresist residuals are removed either by elastic scattering or chemical reactions. However, a potential downside of the process can be an increase in surface roughness by surface modification due to the ion bombardment[6, 7].

In this chapter, we present the results of a study on the effect of plasma etching on SPO plates. We first investigated the possible change in surface roughness with atomic force microscope (AFM) measurements of the plasma etched surfaces. Then we derived the most suitable plasma etching parameters on SPO plates without a photoresist layer. Finally we validated the plasma etching within the coating process on SPO plates with photoresist and proved that it is now compatible with the subsequent bonding step.

3.2 Evaluating the impact of plasma etching on surface roughness

SPO plate surfaces must have a low root-mean-square (rms) roughness (less than approximatively 0.5 nm) to achieve high imaging performance [8–10]. Therefore the first objective is to ensure plasma etching does not increase the surface rms roughness by surface modification due to ion bombardment. For this purpose we performed AFM measurements on nine non-patterned (without photoresist) SPO plates before and after the plasma etching process.

For the plasma etching, the substrates were mounted onto carriers in the coating chamber, as illustrated in Figure 3.1, and exposed to ion bombardment with a mixture of argon and oxygen ions. The plasma discharge power and exposure time vary per sub-

strate and are given in Table 3.1 along with the substrate identification string (id) and the measured rms surface roughness.

AFM measurements were performed in the center of each substrate with scan sizes $1 \times 1\ \mu m^2$ and $20 \times 20\ \mu m^2$. The results obtained are reported in Table 3.1 and show that the rms roughness has decreased, but the change is not significant: 0.25 ± 0.03 nm before plasma etching versus 0.22 ± 0.01 nm after. Plasma etching intensity also has no significant effect on the rms roughness with current condition.

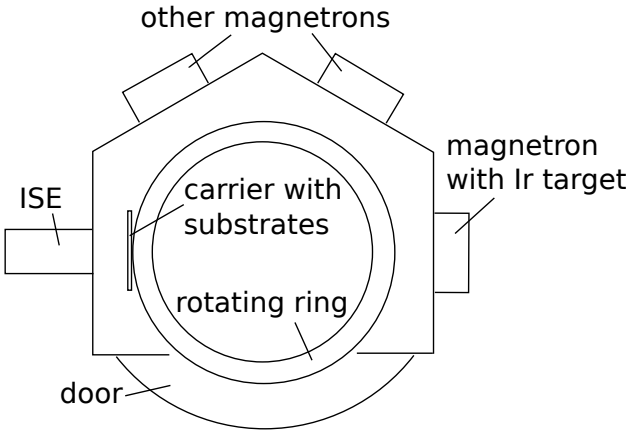

(a)

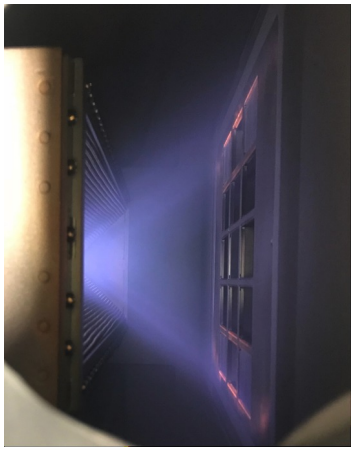

(b)

Figure 3.1: Views of the coating chamber from above. (a) Schematic view displaying the position of the inverse sputter etcher (ISE) compared to the Iridium target and its magnetron. The carriers holding the substrates are mounted on a rotating ring passing by the ISE and the Iridium target successively. Note that two additional magnetrons are available in the chamber and that a door is used to load and unload the carriers. (b) Discharge plasma glow of the ISE. The ISE is visible on the left of the picture and the carriers with the substrates on the right.

Table 3.1: AFM results of nine non-patterned, non-coated SPO plates before and after plasma etching. The plasma discharge power and exposure time vary per substrate. The AFM measurements were performed in the center of each substrates with scan sizes $1 \times 1\ \mu m^2$ and $20 \times 20\ \mu m^2$, respectively.

Substrate id	Discharge power (W)	Exposure time (s)	rms before plasma (nm) $1 \times 1\ \mu m^2$	rms before plasma (nm) $20 \times 20\ \mu m^2$	rms after plasma (nm) $1 \times 1\ \mu m^2$	rms after plasma (nm) $20 \times 20\ \mu m^2$
532-10	100	120	0.25	0.20	0.24	0.19
537-10	100	240	0.25	0.21	0.23	0.20
590-12	100	360	0.28	0.21	0.23	0.21
590-13	450	120	0.29	0.27	0.24	0.21
548-10	450	240	0.25	0.23	0.22	0.21
635-06	450	360	0.25	0.22	0.23	0.22
638-02	800	120	0.27	0.24	0.21	0.22
692-12	800	240	0.26	0.23	0.23	0.23
638-15	800	360	0.28	0.27	0.23	0.24

3.3 Investigating coating stability on non-patterned SPO plates

A 10.0-nm thick Iridium layer (Table 3.2) was deposited on two non-patterned (that is without photoresist), non-plasma-etched SPO plates (substrates 714-10 and 714-11) as well as four non-patterned, plasma-etched SPO plates (substrates 714-01, 714-05, 714-07 and 714-08). The substrates underwent plasma etching with powers 100 W and 450 W, and were thereafter subjected to a wet chemical process (SC-1 cleaning) needed for direct bonding of plates in the complete SPO manufacturing process.

To determine if any damage to the Iridium film occurred during the SC-1 clean, we took two sets of images with an optical microscope, one right after the Iridium deposition and another after the SC-1 clean. The optical microscope images are presented in Figure 3.2. The plasma etching effect is noticeable after the SC-1 clean. Indeed, for the non-plasma etched substrates (i.e. substrate 714-10) numerous holes appear in the Iridium film after the SC-1 clean. The SPO plates plasma etched with a discharge power of 100 W (i.e. substrate 714-01) show an improvement (fewer holes). At a discharge power of 450 W (i.e. substrate 714-07), the plasma etching proved effective at preventing holes in the Iridium film after the SC-1 clean. Note that the holes have a higher density at the edges of the plates.

Results of AFM measurements on the substrates are reported in Table 3.3. The rms roughness of the sputtered Iridium film on non-plasma-etched SPO plates (substrates 714-10 and 714-11, 0.25 ± 0.03 nm) is not significantly different from the rms roughness of the sputtered Iridium film on plasma-etched SPO plates (714-01, 714-05, 714-07 and 714-08, 0.24 ± 0.01 nm).

To assess the impact of SC-1 cleaning on the Iridium coating thickness we also per-

formed X-ray reflectivity (XRR) measurements at 8 keV on the center of the substrates, where the hole density is low for all SPO plates. The data and the best fit models are shown in Figure 3.3, and the best fit thicknesses and roughness are reported in Table 3.3. For the different plasma etching parameters, no significant difference in rms roughness nor thickness of the Iridium films is observed.

We conclude that the thickness and the rms roughness of the sputtered Iridium thin film is not impacted by plasma etching of the non-patterned SPO plates. Plasma etching does however affect the resistance of the coating to SC-1 cleaning, with the higher discharge power of 450 W yielding better results. The higher density of holes at the edges of the plates is attributed to handling of the mirror plates prior to coating; the plates are held on their edges, resulting in possible organic contamination in these areas.

Table 3.2: Parameters for the sputter deposition of 10 nm of Iridium.

Maximum base pressure	2.0×10^{-6} mbar
Working gas pressure	3.4×10^{-3} mbar
Power density	3.1 W cm^{-2}
Target-to-substrate distance	105.0 mm

Table 3.3: AFM and XRR results of two non-plasma-etched SPO plates (substrates 714-10 and 714-11) as well as four plasma etched SPO plates (substrates 714-01, 714-05, 714-07 and 714-08). All substrates are non-patterned, coated with 10 nm of Iridium and have gone through an SC-1 clean. No significant difference in rms roughness nor thickness of the Iridium films is observed.

Substrate id	Discharge power (W)	Exposure time (s)	rms after Iridium coating (nm) 1×1 μm^2	rms after Iridium coating (nm) 20×20 μm^2	XRR fitted thickness (nm)	XRR fitted rms roughness (nm)
714-10	-	-	0.27	0.23	10.1	0.29
714-11	-	-	0.28	0.23	-	-
714-01	100	120	0.24	0.24	10.2	0.29
714-05	100	120	0.25	0.23	-	-
714-07	450	120	0.25	0.23	10.2	0.32
714-08	450	120	0.25	0.24	-	-

3.4 Validating coating stability on patterned SPO plates

The complete SPO manufacturing process includes coating deposition by sputtering thin films of metals onto the non-ribbed side while a photoresist layer prevents the coating from depositing onto the bonding surfaces, enabling direct silicon bonding. This photoresist has a pattern matching the ribs on the backside of the plate (see Figure 3.4). The photoresist is lifted-off chemically in a dimethyl sulfoxide (DMSO) bath after coating deposition and before SC-1 clean.

A layer of 10.0 nm of Iridium was deposited on two patterned (with photoresist), non-plasma-etched SPO plates (substrates 10000-16 and 10005-15) as well as seven pat-

(a)

(b)

(c)

Figure 3.2: Optical microscope images (magnification x5) of substrate corners. Each image shows about 1 mm in the vertical direction and 1.5 mm in the horizontal direction out of the 40.0×65.7 mm^2 substrate surfaces. (a) Substrate 714-10, without plasma etching, (b) substrate 714-01, etched with 100 W and (c) substrate 714-07, etched with 450 W. **Left**, before SC-1 cleaning. **Right**, after SC-1 cleaning. All substrates are non-patterned and coated with 10 nm of Iridium. Fewer holes appear in the Iridium film after the SC-1 clean as the discharge power increases.

terned, plasma-etched SPO plates (substrates 10008-04, 10008-05, 10008-07, 10008-12, 10008-06, 10002-12 and 10008-15). The discharge power of the plasma was 450 W and the exposure time 240 seconds. Subsequently, all substrates went through a lift-off process and then to the SC-1 clean.

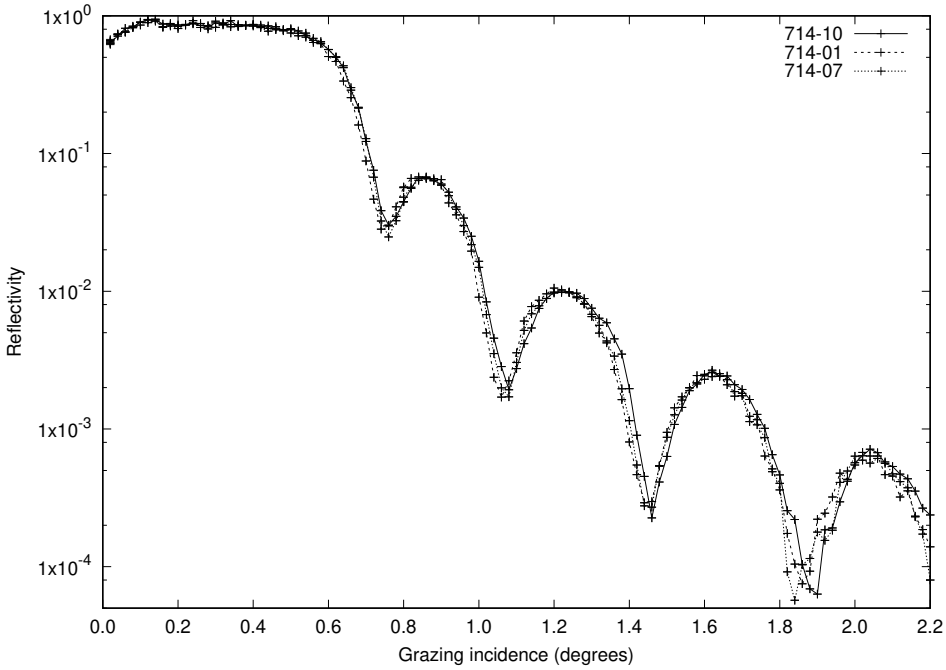

Figure 3.3: Measured XRR of three SPO plates: substrate 714-10 (non-plasma etched), substrate 714-01 (etched with 100 W) and 714-07 (etched with 450 W). All substrates are non-patterned, coated with 10 nm of Iridium and have gone through an SC-1 clean. The rms roughness and thickness of the Iridium films are not significantly different for the different plasma etching powers, resulting in similar XRR.

Figures 3.4 and 3.5 show substrates 10005-15 (without plasma etching) and 10008-04 (with plasma etching) after lift-off (before the SC-1 clean) and after SC-1 cleaning. The Iridium coating has been unintentionally removed on most of the surface of substrate 10005-15 which did not undergo plasma etching (see Figure 3.4). This observation indicates the presence of residual photoresist on the entirety of the reflective side of the patterned SPO plate prior to coating deposition as seen in a previous study[4]. However, the Iridium coating is still present on substrate 10008-04 which underwent plasma etching (see Figure 3.5), indicating that photoresist has been etched by the plasma prior to coating deposition.

In both cases though (with or without plasma etching), the Iridium coating has been unintentionally removed along the edges of the reflective side of the substrates directly after lift-off. The pattern of this coating removal (edges only) supports the hypothesis that photoresist residuals are present in these areas even after plasma etching.

There the resist might be thicker due to edge effects during deposition by spin coating; thickness distribution should be examined and other improved coating method such as spray coating should be considered.

Figure 3.6 shows optical microscope images (magnification x5) of the center of substrate 10008-04 which underwent plasma etching. The interfaces between Iridium coating and silicon oxide are sharp and no holes in the coating are observed. If present, the photoresist residuals on the coating areas (between the patterned stripes) have been etched away by the plasma prior to coating deposition.

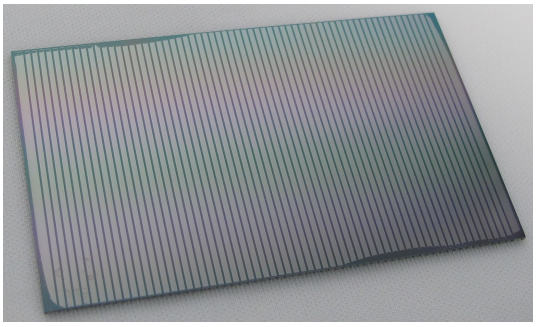

(a)

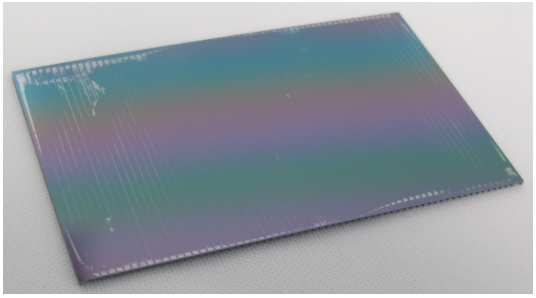

(b)

Figure 3.4: Substrate 10005-15 (without plasma etching). Substrate dimensions are about $40.0 \times 65.7 \times 0.8\ mm^3$. (a) After lift-off, (b) after SC-1 cleaning. The Iridium coating has been unintentionally removed on most of the substrate surface.

3.5 Conclusions and discussion

Plasma etching of SPO plate surfaces before thin film deposition prevents unintentional removal of the metallic coatings during SC-1 cleaning. This indicates that the substrates have photoresist residuals and/or organic contamination on the reflective side. Indeed the plasma etching process performed by bombarding the SPO plate surface with a mixture of argon and oxygen ions would remove, if present, photoresist residuals and organic contamination by elastic scattering and/or chemical reactions. Most of the organic contamination and some of these residuals have been removed successfully by plasma etching with a discharge power of 450 W prior to coating deposition but not in the regions close to the edges. There, photoresist residuals might be thicker due to the spin

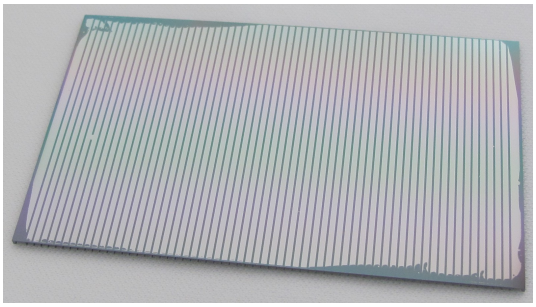

(a)

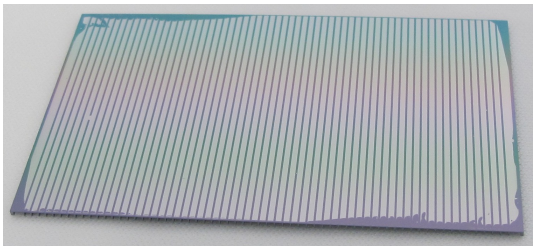

(b)

Figure 3.5: Substrate 10008-04 (with plasma etching). Substrate dimensions are about $40.0 \times 65.7 \times 0.8$ mm^3. (a) After lift-off, (b) after SC-1 cleaning. The Iridium coating is unaffected by the SC-1 clean based on visual inspection.

coating deposition method used. We recommend to measure the thickness distribution of the photoresist layer and to consider spray coating. Also, it would be interesting to perform direct measurement of the organic contamination, for instance by using X-ray photoelectron spectroscopy.

It is also concluded that plasma etching and thin film deposition do not impact the surface rms roughness, allowing for low scattering and high imaging performance from the coated SPO plates.

Overall, this work demonstrates that plasma etching makes the metallic coating deposition process compatible with the SC-1 cleaning step needed for direct silicon bonding. This is essential to increase the effective area of SPO-based X-ray telescopes like Athena, to build complex shapes such as Wolter type-I that will survive launch and space flight conditions, and therefore to extend the breadth and scope of future astrophysical observations.

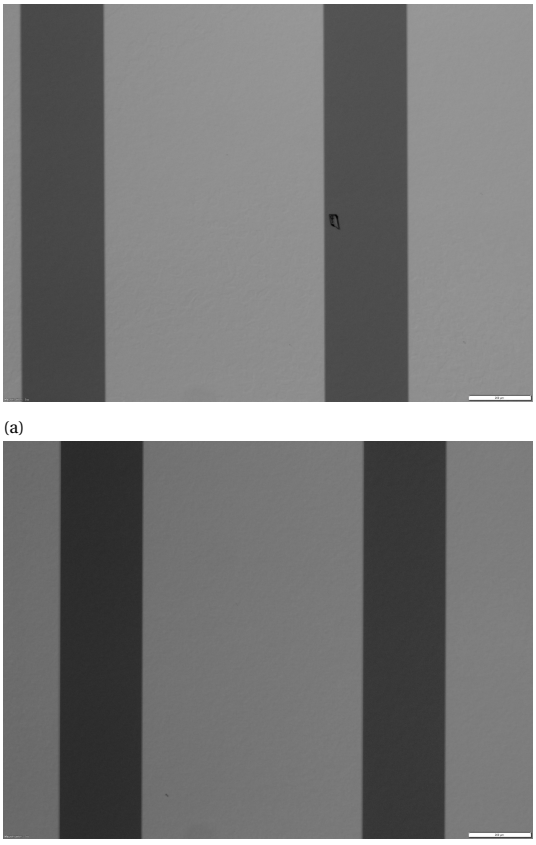

(a)

(b)

Figure 3.6: Optical microscope images (magnification x5) of the surface of substrate 10008-04 (with plasma etching). (a) After lift-off, (b) after SC-1 cleaning. In both cases the interfaces between Iridium coating (light grey) and silicon oxide (dark grey, 270 μm in the horizontal direction) are sharp and no holes are observed in the coating.

References

[1] D. Girou, S. Massahi, D. D. M. Ferreira, *et al.*, *Plasma etching for the compatibility of thin film metallic coatings and direct bonding of silicon pore optics,* Journal of Applied Physics **128**, 095302 (2020), https://doi.org/10.1063/5.0010212 .

[2] D. D. M. Ferreira, F. E. Christensen, A. C. Jakobsen, *et al.*, *ATHENA optimized coating design,* in *Space Telescopes and Instrumentation 2012: Ultraviolet to Gamma Ray*, Vol. 8443, edited by T. Takahashi, S. S. Murray, and J.-W. A. den Herder, International Society for Optics and Photonics (SPIE, 2012) pp. 1601 – 1611.

[3] W. KERN, *Cleaning solutions based on hydrogen peroxide for use in silicon semiconductor technology,* RCA Review **31**, 187 (1970).

[4] S. Massahi, D. A. Girou, D. D. M. Ferreira, *et al.*, *Investigation of photolithography process on SPOs for the Athena mission,* in *Optics for EUV, X-Ray, and Gamma-Ray Astronomy VII*, Vol. 9603, edited by S. L. O'Dell and G. Pareschi, International Society for Optics and Photonics (SPIE, 2015) pp. 155 – 165.

[5] S. Massahi, F. E. Christensen, D. D. M. Ferreira, *et al.*, *Installation and commissioning of the silicon pore optics coating facility for the ATHENA mission,* in *Optics for EUV, X-Ray, and Gamma-Ray Astronomy IX*, Vol. 11119, edited by S. L. O'Dell and G. Pareschi, International Society for Optics and Photonics (SPIE, 2019) pp. 91 – 106.

[6] S. C. Vitkavage and E. A. Irene, *Electrical and ellipsometric characterization of the removal of silicon surface damage and contamination resulting from ion beam and plasma processing,* Journal of Applied Physics **64**, 1983 (1988).

[7] R. Pétri, P. Brault, O. Vatel, *et al.*, *Silicon roughness induced by plasma etching,* Journal of Applied Physics **75**, 7498 (1994).

[8] J. Stover, *Optical Scattering: Measurement and Analysis*, Press Monographs (SPIE Press, 2012).

[9] D. Spiga, G. Cusumano, and G. Pareschi, *HEW simulations and quantification of the microroughness requirements for x-ray telescopes by means of numerical and analytical methods,* in *Optics for EUV, X-Ray, and Gamma-Ray Astronomy III*, Vol. 6688, edited by S. L. O'Dell and G. Pareschi (SPIE, 2007) p. 66880H.

[10] D. Spiga, *Optical module HEW simulations for the X-ray telescopes SIMBOL-X, EDGE and XEUS,* in *Optics for EUV, X-Ray, and Gamma-Ray Astronomy III*, Vol. 6688, edited by S. L. O'Dell and G. Pareschi (SPIE, 2007) p. 66880K.